Flood Monitoring in Khammam: Leveraging Multi-Temporal Synthetic Aperture Radar and Geospatial Techniques to Assess Land Use Impacts

Veena Raparthi[1], Durgesh Kurmi[2*], Kethoori Venkatesh[3]

[1]Assistant Professor, Osmania University, Hyderabad, Telangana, India
[2]Assistant Professor, Govt. Model College, Damoh, M.P., India
[3]Assistant Professor, Nizam College, Hyderabad, Telangana, India

Received:22 July 2025
Accepted:04 August 2025
Genre: Geography

Corresponding Author
Dr. Durgesh Kurmi,
durgeshdavv@gmail.com

Cite this article
Raparthi, V., Kurmi, D., Venkatesh, K., (2025). Flood Monitoring in Khammam: Leveraging Multi-Temporal Synthetic Aperture Radar and Geospatial Techniques to Assess Land Use Impacts. JESS, 1(1), 9-23.

ABSTRACT

Floods in India annually result in numerous fatalities and substantial economic damage, making flood monitoring essential for understanding their patterns and characteristics to aid in mitigation efforts. This study investigates the impact of extreme rainfall events at the Khammam district. Some areas in Khammam received over 20cm of one-day rainfall, resulting in substantial Inundation of 100 villages, cropland and 5 fatalities. The research aims to Map the flood event using Sentinel-1 SAR data and quantify the impact on different land cover classes.

The study used Sentinel-1 Synthetic Aperture Radar (SAR) data and Google Earth Engine (GEE) to map and analyze flood inundation patterns. SAR is crucial for flood hazard mapping and monitoring because it can image the Earth's surface regardless of weather conditions or time of day. The findings show that 25684 hectares of land were inundated, representing 5.7% of the study area, with croplands being the most affected (24710 hectares), followed by rangeland (138.39 hectares). Built-up areas also experienced inundation, affecting 154 hectares of infrastructure.

The study highlights the vulnerability of agricultural livelihoods to extreme weather events and underscores the importance of using remote sensing technologies like SAR for accurate and timely flood monitoring. The insights from this research can inform better flood management and mitigation strategies, emphasizing the need for effective disaster management, Climate Resilient planning, and sustainable agricultural practices.

Keywords: Flood Inundation, Sentinel-1 SAR, Google Earth Engine, Land Use Land Cover and Disaster Management,

1. Introduction

Floods cause the most devastating effects all over the world among all disasters. About 90% of world disasters are water-related, with 43% occurring between 1997 and 2017, according to a UN report 2015. 1.81 billion people, which is equivalent to 23% of the global population, are at direct risk of flooding. (Amitrano et al., 2024). It is projected that global economic losses caused by flooding will increase by 17% over the next 20 years (Uddin et al., 2019). Many studies have indicated that global warming could increase the likelihood of flooding, especially in flood-prone areas (Li et al., 2023). According to Disaster Management of India Report 2010, out of 40 million hectares of flood-prone area in the country, on average, floods affect an area of around 7.5 million hectares per year. In 2020, flooding was responsible for the 3rd deadliest event of the year costing 1,922 lives, with an estimated economic loss of 7.5 billion US$ (Sarkar, 2022). The financial and human losses from flooding have been increasing at a rate of 6.3% and 1.5% per year, respectively, over the last fifty years (NDMA, 2010).

India, with its diverse topography and climatic conditions, is particularly vulnerable to floods. Approximately 12% of the country's land area is prone to flooding, affecting nearly 75 million people annually (Rahman & Thakur, 2018). In India, the major river systems such as the Ganges, Brahmaputra, and their tributaries are often in spate during the monsoon season, leading to severe floods in the northern and northeastern states (Agnihotri et al., 2019). The 2018 Kerala floods and the 2020 Assam floods are recent examples of the severe impact of these events on local communities and economies (Moothedan et al., 2020).

The River Godavari and its tributaries are the longest of the peninsular rivers and account for nearly 9.5% of the total geographical area of India. The lower reaches and coastal areas of its basin are prone to cyclones and floods. The Krishna River basin is an interstate basin located in Peninsular India. It is the fourth largest river basin in the country, covering an area of 258949 km². Most of the rainfall in the basin occurs during the southwest monsoon season, which lasts from June to September. However, recent analyses of monthly rainfall data indicate that significant rainfall contributions have also been observed in October (Pakhale et al., 2023). The entire study area basin slopes toward the floodplains to the south, which are very flat and often experience inundation. The Krishna and Godavari basin of Telangana frequently experiences severe floods, particularly during the monsoon season, resulting in significant loss of life and property (Sarkar, 2022).

Around the world, floods occur unpredictably, making it difficult to measure hydraulic factors like water level and discharge during flood events (Agnihotri et al., 2019). In times like these, traditional ways of getting information are difficult due to damage to communication and transportation systems. Remote sensing technology provides real-

time and reliable information for assessing flood damage. Several remote sensing satellites collect extensive spatial data used for near real-time flood inundation mapping and monitoring (Amitrano et al., 2024). Multispectral satellites cannot be used to monitor floods when there is extensive cloud cover. However, synthetic aperture radar (SAR) sensors are particularly valuable due to their all-weather and all-time imaging capabilities compared to optical satellite sensors. Many scholars have utilized microwave remote-sensing datasets for continuous flood monitoring and mapping in different parts of the world (Li et al., 2023; Qiu et al., 2021; Tazmul Islam & Meng, 2022; Uddin et al., 2019; Wu et al., 2023; H. Zhang et al., 2021). (Vekaria et al., 2023) (Moothedan et al., n.d.-b). (Amitrano et al., 2024) reviewed various SAR techniques and datasets for flood detection, highlighting their global applicability. Studies such as (Uddin et al., 2019) have shown the rapid and accurate flood mapping capabilities of SAR data in different regions. The integration of SAR data into flood monitoring systems significantly enhances the ability to manage and mitigate flood impacts, providing crucial data even in challenging conditions where conventional methods fail. The analysis of the spatial extent of flood inundation from remotely sensed imagery is crucial for flood mitigation and management. Knowledge of the spatial extent of extreme flooding is valuable for decision-makers and disaster relief agencies, as it helps them efficiently provide immediate and lasting support to populations affected by flood events (Rahman & Thakur, 2018b).

2. Study Area

The study area encompasses the Khammam districts, situated in the Eastern region of Telangana state which comes under Kaleshwaram Zone 1, India. It is located between 16°70’ and 17°60’ North latitude and 79°80’ and 80°90’ East longitude, total area of 4491 sqkm (Figure 1). The region experiences semi-arid climatic conditions, with an average south west monsoon rainfall of 913 mm. About 90% of the rainfall occurs during the southwest monsoon, with the highest mean monthly rainfall observed in July. The elevation profiles range from less than 18m to more than 700m above sea level, decreasing as one moves southward due to the presence of the Munneru River basin tributary of Krishna along its centre which has a 9854 sqkm drainage area. Major water bodies present in this basin are Pakhal Lake, Wyra Reservoir, Bhayyaram Cheruvu, and Lanka Sagar Reservoir. In this basin, red soils predominate, followed by black soils. Two-thirds of the basin is made up of agricultural land. The three main crops grown in this area are maize, cotton, and paddy. The total drainage area of the basin is 9854 km^2.

The Khammam district has 21 mandals and 589 panchayats with a population of 14,01,369. It is the district with About 50% of the area is agriculture sown, and the population density is 312 people per sqkm. This study aims to investigate the flood event in Rural Eastern Telangana, India, using multi-temporal Sentinel-1 SAR data. The objectives of this research are:

- To map the spatial extent and temporal dynamics of the flood event using Sentinel-1 SAR data.
- To quantify the impact of the flood on different land cover classes by integrating SAR-derived flood maps with high-resolution Land Use Land Cover data.
- To provide insights into the vulnerability of agricultural livelihoods in the region to extreme weather events.

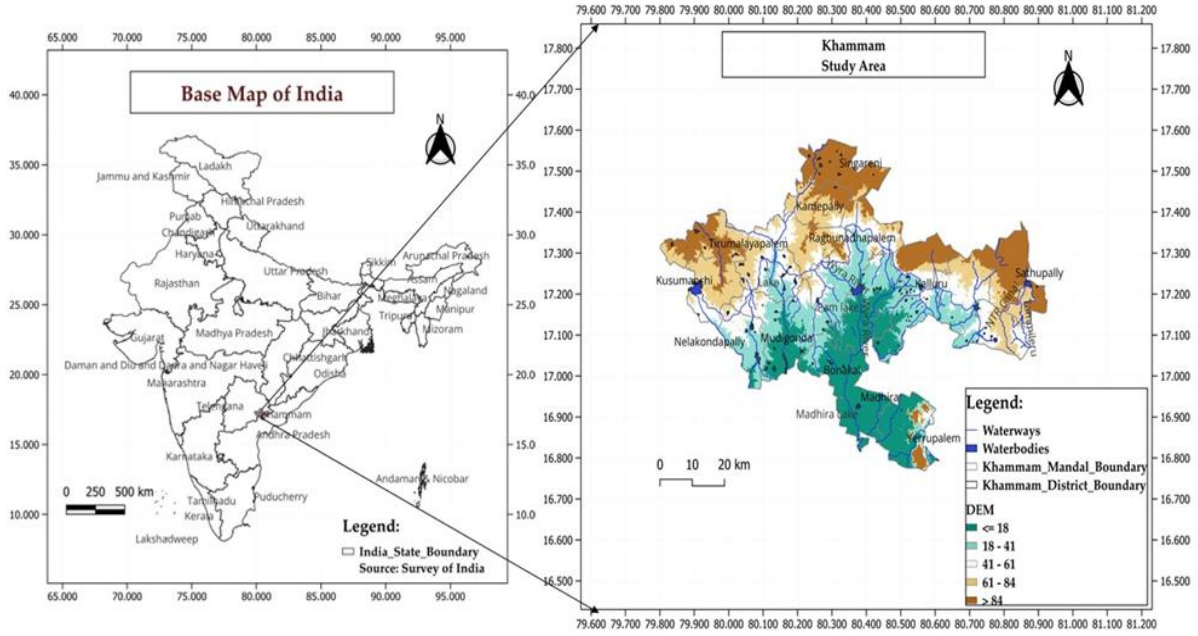

Figure 1: Study Area – Khammam

3. Datasets

The research extensively employs datasets from the Google Earth Engine Data Catalog. Various types of datasets are utilized, including study area shapefiles, SAR (Sentinel-1) images, topography data, rainfall data, and elevation data. The study area boundary in vector data format and July Rainfall data of 20 ground stations, were obtained from the Telangana open data portal, The study area, encompassing Mulugu and Jayashankar Bhupapally, was extracted from the original Telangana state boundary data and then exported as a shapefile to represent the study area geometry within Google Earth Engine. The open-access Sentinel-1 SAR C-band dataset has a high resolution of 10 meters (5x20m) (Table 1).

Pre-processing of Sentinel's ground range detected (GRD) products is provided in the GEE platform has been completed. The cross-polarized (VH) channels were acquired as Level-1 GRD products. VH polarizations were utilized for flood mapping in this research (Google Earth Engine)

The WWF HydroSHEDS Void-Filled DEM (90m), 3 Arc-Seconds within the GEE data catalog, was also utilized. This void-filled elevation dataset serves as the first step toward producing conditioned DEM datasets (Table 1). Additionally, the global surface water

layer from JRC was used to identify permanent and semi-permanent water bodies within the study area. This dataset is also available within the GEE platform (Google Earth Engine). Annual global maps of land use and land cover (LULC) have been updated to version 3 with data ranging from 2017 to 2023. These maps are based on 10m resolution ESA Sentinel-2 imagery. Each map represents a composite of LULC predictions for 9 classes throughout the year. The dataset was created by Impact Observatory, utilizing billions of human-labeled pixels curated by the National Geographic Society to train a deep-learning model for land classification. Each map has been assessed to have an average accuracy of over 75% (Esri data portal).

Table 1: Data Sets

S/N	Data Set	Year	Resolution	Band	Source
1	Sentinel 1A SAR	2024/08/20 - 2024/08/31 Before Flood	10m	C Band (VV & VH)	Copernicus ESA-GEE
2	Sentinel 1A SAR	2024/09/01-2023/09/07 After Flood	10m	C Band (VV & VH)	Copernicus ESA-GEE
3	Sentinel 2 LULC	-	10m	-	ESRI - LULC
4	SRTM Void-Filled DEM	2000	90m	DEM	SRTM - GEE
5	JRC Global Surface Water	2022	30m	GSW	Landsat - GEE
6	Rainfall Data	Aug and Sep 2024	21 Ground stations	-	Telangana Open Data Portal
7	Shapefile	-	-	-	Telangana Open Data Portal

4. Methodology

The Sentinel-1 C-band (SAR) sensor can effectively observe surface and shallow subsurface features. This study utilized the capabilities of Sentinel-1 Synthetic Aperture Radar data and Google Earth Engine to map and analyze flood inundation patterns in the Khammam districts accurately. The data was collected using Google Earth Engine, a platform for processing large datasets. The area of interest (AOI) was the Khammam district, with two periods: Before flood and After flood. The dates for SAR imagery acquisition were strategically selected based on significant rainfall events recorded. Notably, most areas experienced their highest one-day rainfall on September 01, 2024, accompanied by substantial monthly totals, which indicated potential flooding. To monitor flood dynamics effectively, data from August 20 to August 31, 2024, were utilized as before flood baselines (Figure 2), while data from September 01 to September

07, 2024, captured after flood conditions (Figure 3), as determined by ground-based station data from August and September. For identifying areas with high rainfall, IDW (Inverse Distance Weighting) maps were generated for September specifically for Sep 01st, 2024.

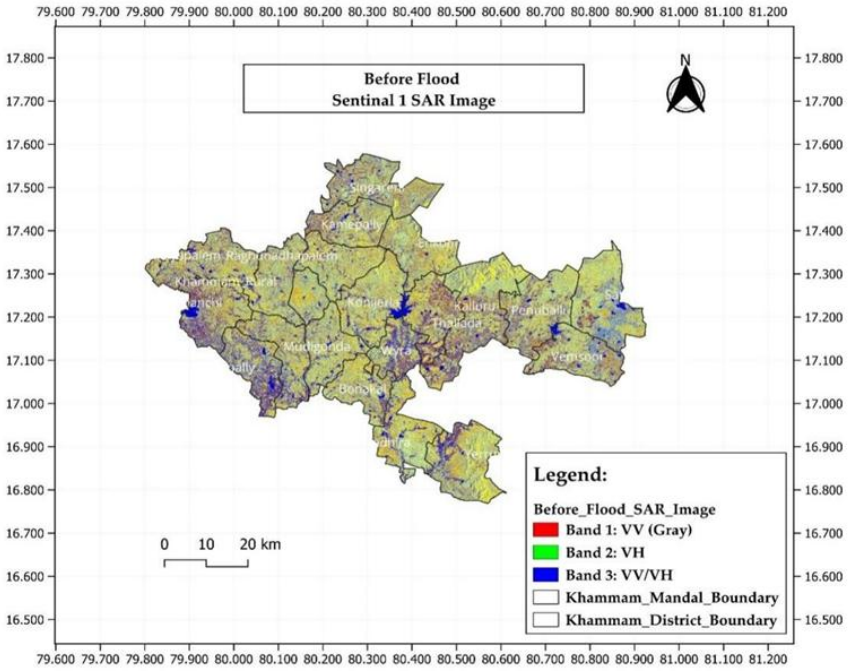

Figure 2: Before Flood SAR Image

The study used Interferometric Wide Swath (IW) mode and VH polarization in Descending orbit, which is highly sensitive to changes in surface roughness and can distinguish between water and non-water surfaces (Amitrano et al., 2024). Operating at a frequency of 5.405 GHz, the C-band strikes a balance between penetration depth and surface detail. The original polarization of VH and VV were used for analysis in GEE and calculated in VV/VH combinations. The VH cross-polarization band was used to extract water information due to the complexity of land covers, interference of mountainous shadows, and the large proportion of small-scale water bodies (L. Zhang & Xia, 2022). VV polarisation treats partially submerged features as coded, leading to a greater inundation extent compared to VH polarisation. In contrast, VH polarisation offers a broader range of backscatter values on surfaces covered with vegetation (Vekaria et al., 2023).

The data was pre-processed by mosaicking and clipping images from the pre-flood and post-flood periods, threshold value of 1.25 was applied to the ratio image to identify flooded areas (Figure 4). Pixels with values above this threshold were classified as flooded and then processed using a Refined Lee Speckle Filter to reduce speckle noise and preserve edges. The images were converted from decibel scale to natural units before filtering and back to dB scale post-filtering (Agnihotri et al., 2019).

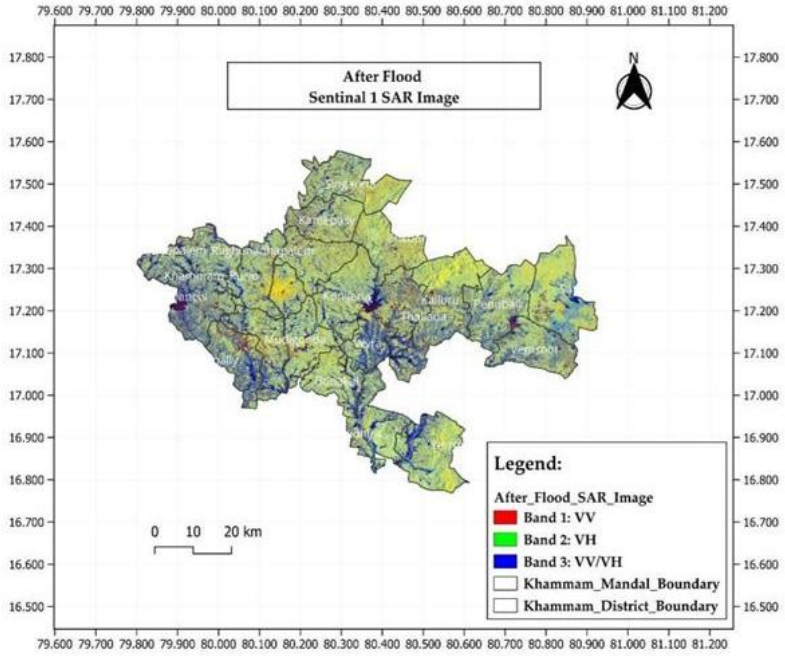

Figure 3: After Flood SAR Image

The SRTM Void-Filled DEM (90m), 3 Arc-Seconds data was utilized for range-Doppler terrain correction and used JRC global surface water(30m) extent for identification of permanent water bodies areas with seasonality values of 3 or higher were masked out from the detected flooded areas to exclude these from the analysis (UN-SPIDER Knowledge Portal) (Figure 4). The noise was removed and the image was calibrated, followed by binarization using a specific threshold value. Water pixels exhibit a very low backscatter coefficient and appear darker due to the specular nature of water against microwave signals. These darker pixels were extracted from the SAR data using a threshold value selected from the data's histogram.(Amitrano et al., 2024). Results were visualized using a color-coded map and a histogram of the flooded areas to provide a distribution of flood extent.

The land use and land cover of the study area were derived from the ESRI land cover data for the year 2023. Intersecting the flooded Water pixel with the LULC in the QGIS environment helps in the segmentation of different land cover types based on whether a pixel was covered by buildings, vegetation, or barren land, and then further subdivided into 7 classes. This data shows both flooded and non-flooded areas of different types of land cover (LULC) (Wang et al., 2022).

This methodology presents an effective approach to flood detection using Sentinel-1 SAR imagery, Land Use Land Cover (LULC) data, Google Earth Engine, and QGIS. It provides valuable information on inundation classified by land cover type for each administrative region, which aids in disaster management, response, and future flood mitigation planning.

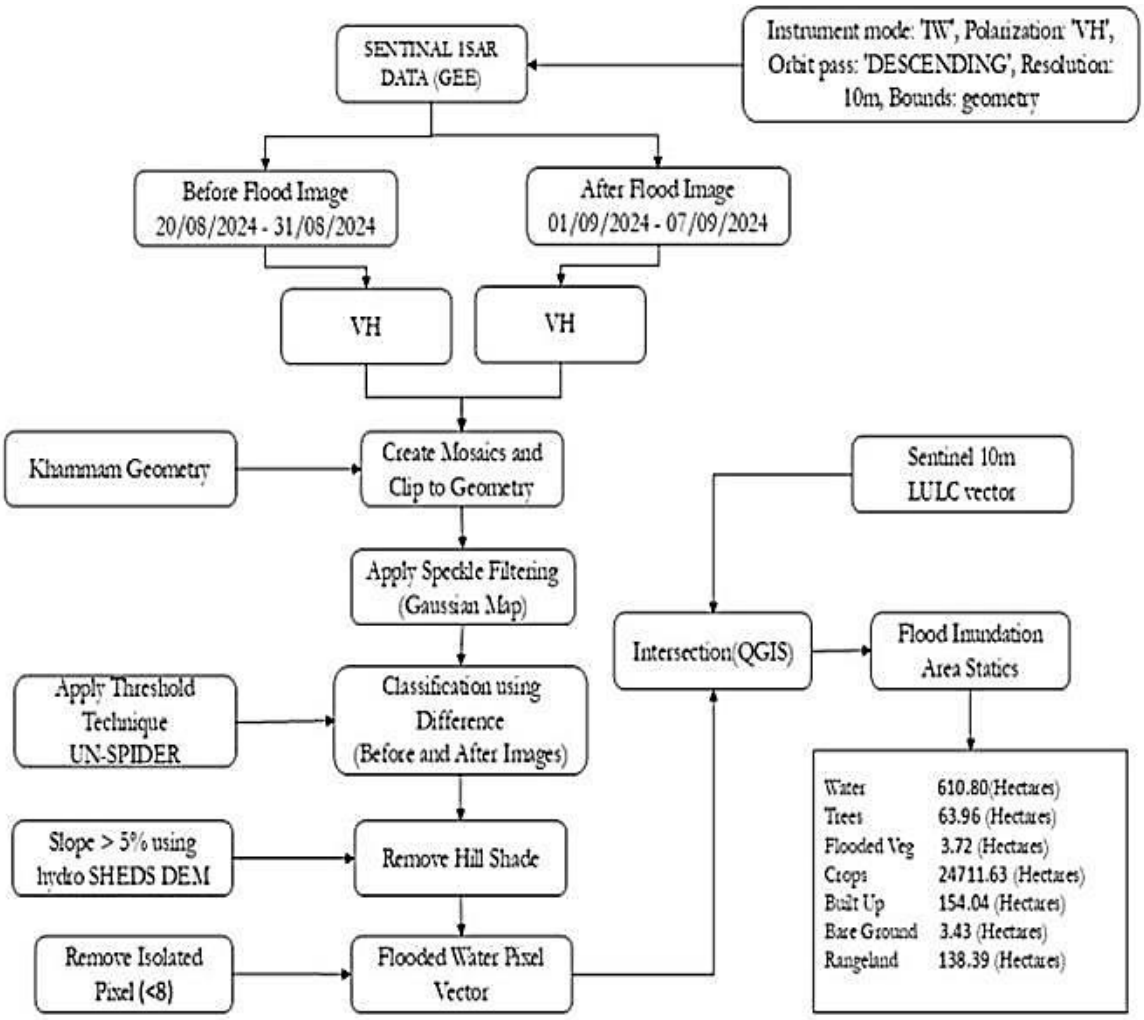

Figure 4: Flow Chart

5. Results & Discussion

5.1 Land Use and Land Cover: Khammam District in southern India is a diverse agricultural and land use landscape, with a total land area of 4,491.06 sq. km. (Table 2). The district is largely agricultural, with cultivation representing 78.3% of the land. The remaining areas include built-up regions, tree-covered regions or forests, rangelands, water bodies, and minimal sections of bare ground and flooded vegetation (Figure 5).

Agriculture in Khammam is divided primarily between the Kharif (monsoon) and Rabi (winter) cropping seasons, with paddy and cotton as the dominant crops. The Kharif season features a significant portion of paddy cultivation, accounting for approximately 39.63% of the district's cropped area, while cotton occupies 35.93%. In the Rabi season, paddy remains a critical crop, comprising 66.56% of the area under cultivation, while maize covers about 23.16%. Other Rabi crops include green gram, chilies, and sugarcane, grown in small portions.

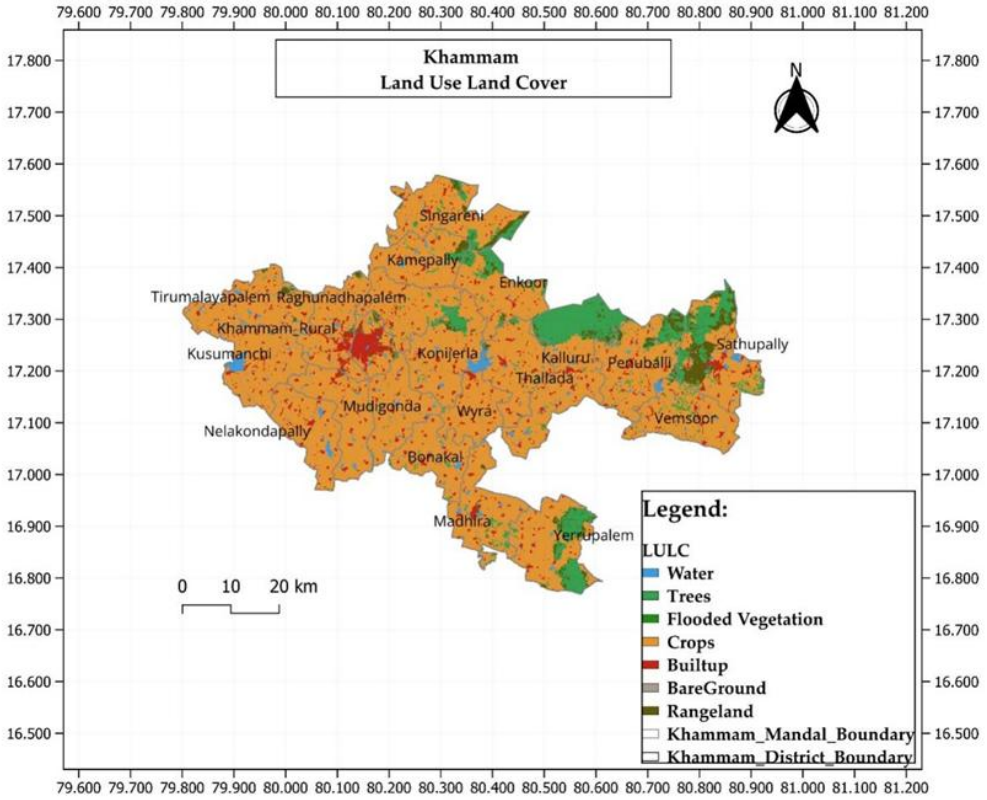

Figure 5: LULC of Study Area

Table 2: LULC Area

Sr. No.	Class	Area (Sq. km)
1	Bare ground	0.697
2	Built-up	274.008
3	Crops	3514.824
4	Flooded Vegetation	0.185
5	Rangeland	148.641
6	Trees	433.946
7	Water	118.758
	Total	**4491.059**

The distribution of landholdings in Khammam is skewed towards small and marginal farmers, with marginal farmers owning less than 2.47 acres constituting the majority of landholders. Small farmers with holdings between 2.47 and 4.93 acres cover about 28% of the area, while semi-medium farmers account for another 23%. Medium-sized farms (9.88 to 24.7 acres) and large holdings, though minimal in number, occupy the remaining agricultural area. Water resources in Khammam support a complex irrigation network, featuring major, medium, and minor irrigation projects. Major irrigation projects, such as

the NSP Left Canal, support extensive paddy cultivation, while medium projects, like the Wyra project, support cotton and other water-efficient crops.

5.2 Rainfall: The average annual rainfall in Khammam is 913 mm (Figure 6).

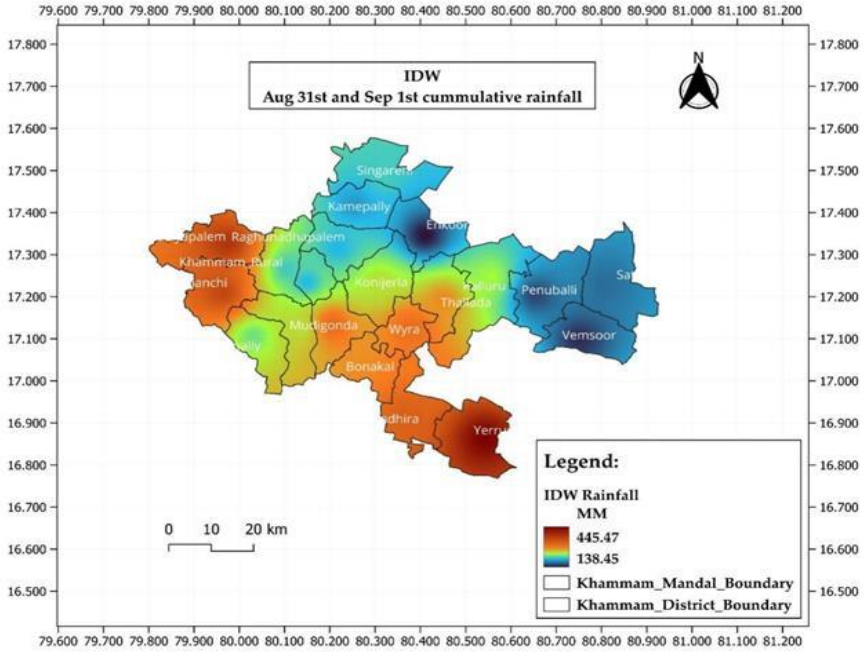

Figure 6: IDW Map of Rainfall

Approximately 90% of the rainfall happens during the monsoon season in the southwest. Data from ground stations in the 21 mandals of Khammam shows significant variability in August and September rainfall and the highest one-day rainfall (Figure 7 and Figure 8). Most of the mandals, experience more than 20% of their annual rainfall in just one day, and few mandals have recorded 40% of rainfall just in 2 days i.e., August 31st and September 1st.

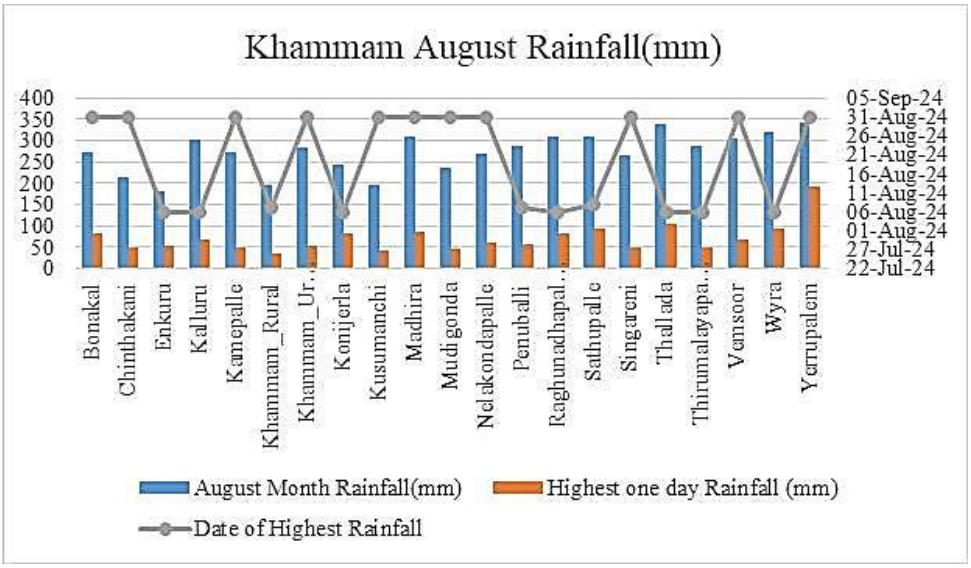

Figure 7: August Rainfall

The highest one-day recorded rainfall was 330mm in Thirumalayapalem and 315mm in Kusumanchi (SI Table 1), these record rainfall regions, namely are in the south and west regions of the districts, which could lead to high inundation. It is noteworthy that most of the regions are located along the Munneru River stream.

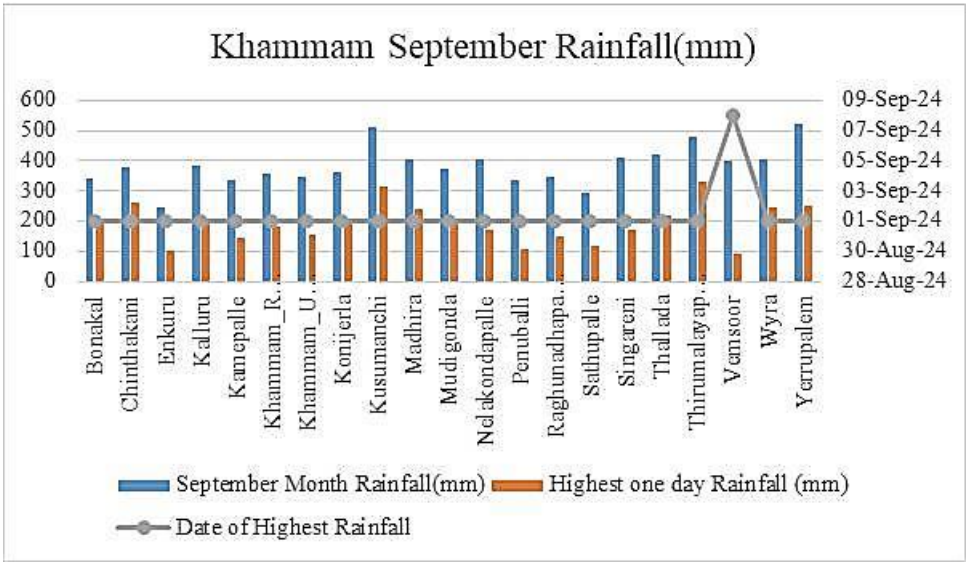

Figure 8: September Rainfall

5.3 Flooded Inundation Area: Flooding is a significant challenge in land and water management, particularly in rural and agricultural areas. This report assesses flood inundation impacts across different land classes. The dataset used for this analysis is derived from the JRC Global Surface Water (GSW) extent data, providing detailed mapping of surface water distribution over time. By isolating water bodies that persisted for over one month, a more accurate delineation of flood inundation was achieved, separating stable water sources from those formed due to recent flooding.

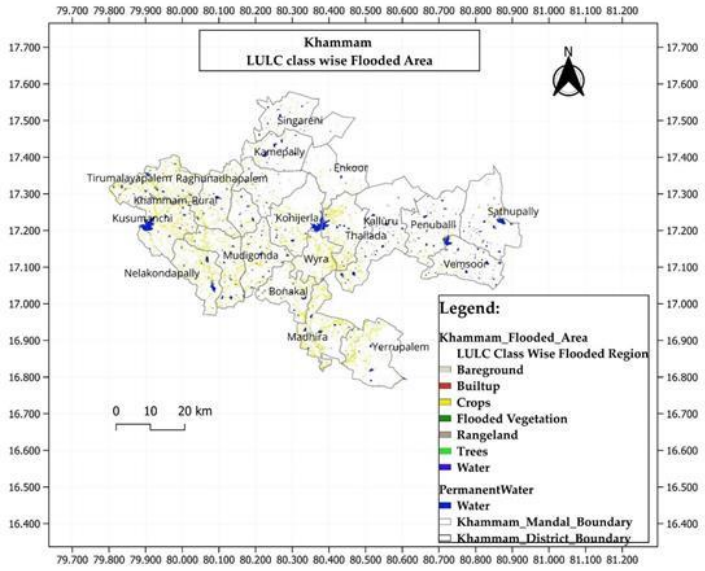

Figure 9: Flooded Area Map

The flooded area totaled 25,684.28 hectares, affecting crops, rangelands, forested areas, and built-up regions, disrupting local livelihoods, infrastructure, and agricultural activities (Figure 9). A total of 108 square kilometers of permanent water bodies were identified, helping to refine the inundation analysis by removing stable water sources from the temporary flood extent.

The flood inundation affected multiple land classes, each impacted to varying degrees. Bare ground areas experienced minimal flooding, while built-up areas experienced 154.03 hectares of inundation, constituting 0.6% of the total flooded area. The agricultural sector was the most affected, accounting for 24,710.06 (Table 3) hectares or 96.21% of the total inundated area. Flooded vegetation areas experienced a limited impact, with only 3.72 hectares submerged, representing 0.014% of the total flooded area. Rangelands faced moderate flooding, with 138.39 hectares (0.54% of the flooded area) affected (Table 3).

Table 3: Flooded Area

S. No	Class	Flooded Area (Hectares)	Percentage
1	Bare ground	3.43	0.013
2	Built-up	**154.03**	0.600
3	Crops	**24710.06**	**96.207**
4	Flooded Vegetation	3.72	0.014
5	Rangeland	**138.39**	0.539
6	Trees	63.97	0.249
7	Water	610.68	2.378
	Total	**25684.28**	**100**

Trees/forested areas experienced flooding, impacting 63.97 hectares or 0.25% of the total inundated area. Water bodies accounted for 610.68 hectares (2.38%) of the flooded area, including permanent and seasonal water bodies impacted by excess floodwater. The JRC GSW data was used to exclude areas already identified as stable or permanent water bodies, totaling 108 sq km, to provide a more accurate flood inundation analysis.

5.4 Flood Analysis: The flood analysis of Khammam District indicates that croplands are the most affected LULC category, with an inundated area totalling 24,710.06 hectares and constituting 96.21% of the district's flooded land. Significant impacts are seen in Madhira (2,871.53 ha), Tirumalayapalem (2,617.90 ha), and Kusumanchi (2,334.88 ha), highlighting the vulnerability of these agricultural areas to flood events and the resulting risks to food security and livelihoods (Figure 10).

Built-up areas in Khammam Rural and Urban mandals also face notable flooding, with 27.43 ha and 26.87 ha affected, respectively (SI Table 2). This poses a risk of infrastructure damage in both rural and urban settings, with the more developed areas in Khammam Urban particularly susceptible. Protecting these areas is essential to maintaining public

services and minimizing disruption to residents in the event of future floods.

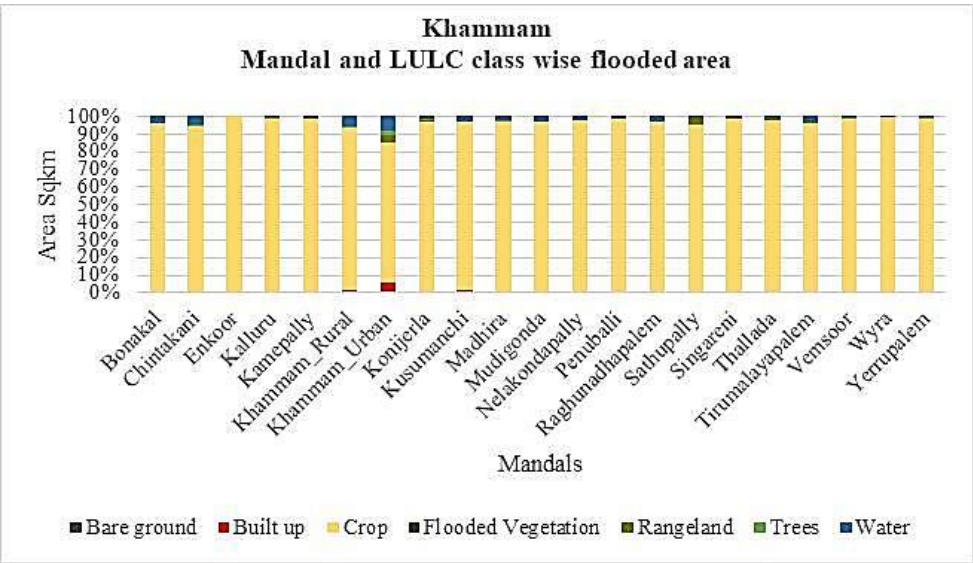

Figure 10: LULC Class wise flooded area

Flooding impacts rangelands and tree-covered areas as well, although to a lesser extent than croplands. Notable rangeland inundation is recorded in Tirumalayapalem (36.01 ha) and Thallada (21.83 ha), affecting grazing areas and natural vegetation, which are crucial for local biodiversity. Tree-covered areas such as Madhira (17.45 ha) and Khammam Urban (10.43 ha) also experience flooding, potentially impacting the region's ecosystems.

Overall, Madhira, Tirumalayapalem, and Kusumanchi contribute the highest flood-affected area percentages, with 11.63%, 10.68%, and 9.48% respectively. These findings highlight the urgent need for targeted flood management measures, particularly in cropland areas, to protect the district's agricultural and ecological resources. Sustainable land management and flood resilience strategies are critical to preserving the stability of Khammam's rural economy and landscapes amidst frequent flood events.

6. Conclusion

The extensive flooding of agricultural lands highlights the vulnerability of the Agrarian economy to flood events, leading to economic losses and food security issues. The inundation of rangelands and water bodies indicates potential long-term environmental consequences and flooding in built-up areas stresses the importance of resilient infrastructure to support sustainable development and disaster risk reduction, emphasizing the importance of resilient infrastructure for sustainable development and disaster risk reduction.

Recommendations include disaster management, policy and planning, agriculture support, infrastructure development, and community engagement. Implementing disaster management guidelines focusing on mitigation and relief is crucial, as is enhancing early

warning systems, promoting disaster-resilient infrastructure, and ensuring effective relief and recovery operations. Enforcing flood plain planning and building zonation regulations can help mitigate flood risks. Providing targeted support to farmers and promoting sustainable agricultural practices can enhance resilience. Building disaster mitigation infrastructure through schemes like MGNREGA can protect vulnerable areas. Engaging local communities in disaster preparedness and response activities can improve resilience and ensure the sustainability of interventions.

Future studies should aim to incorporate more granular data and explore the socio-economic implications of flooding in greater detail. Longitudinal studies are needed to assess the long-term impact of flooding on various land use categories and communities. Overall, comprehensive flood management strategies, effective policy implementation, and community engagement are essential to mitigate the adverse effects of flooding and enhance the resilience of vulnerable regions.

Author Contributions

Dr. Veena Raparthi- conceived and planned the experiments, Writing
Durgesh Kurmi- Data Collection, Formal Analysis and Interpretation
Kethoori Venkatesh- Writing, contributed to the final manuscript.

Funding Sources

No funding or support was received from organizations that may gain or lose financially through this publication.

Acknowledgement

The authors would like to express their sincere gratitude to Osmania University; Principal, Govt. Model College Damoh and Principal, Nizam College, Hyderabad for their kind permission and support contributed to the successful completion of this research work.

Statement of Conflict of Interest

The authors declare that there is no conflict of interest regarding the publication of this research paper. The authors have no financial, commercial, or personal relationships that could be perceived to influence the work reported in this paper.

References

1. Agnihotri, A. K., Ohri, A., Gaur, S., Shivam, Das, N., & Mishra, S. (2019). Flood inundation mapping and monitoring using SAR data and its impact on Ramganga River in Ganga basin. Environmental Monitoring and Assessment, 191(12). https://doi.org/10.1007/s10661-019-7903-4
2. Amitrano, D., Di Martino, G., Di Simone, A., & Imperatore, P. (2024). Flood Detection with SAR: A Review of Techniques and Datasets. In Remote Sensing (Vol. 16, Issue 4). Multidisciplinary Digital Publishing Institute (MDPI). https://doi.org/10.3390/rs16040656
3. https://data.telangana.gov.in/dataset/telangana-panchayat-raj-rural-development-panchayat-wise-building-permission-data
4. https://developers.google.com/earthengine/datasets/catalog/COPERNICUS_S1_GRD
5. https://developers.google.com/earthengine/datasets/catalog/WWF_HydroSHEDS_03VFDEM
6. https://developers.google.com/earthengine/datasets/catalog/WWF_HydroSHEDS_03VFDEM
7. (Esri data portal) | Sentinel-2 Land Cover Explorer (arcgis.com))
8. Li, H., Xu, Z., Zhou, Y., He, X., & He, M. (2023). Flood Monitoring Using Sentinel-1 SAR for Agricultural Disaster Assessment in Poyang Lake Region. Remote Sensing, 15(21). https://doi.org/10.3390/rs15215247
9. Moothedan, A. J., Thakur, P. K., Garg, V., Dhote, P. R., Aggarwal, S. P., & Mohapatra, M. (2020). AUTOMATIC FLOOD MAPPING USING SENTINEL-1 GRD SAR IMAGES AND GOOGLE EARTH ENGINE: A CASE STUDY OF DARBHANGAH, BIHAR.

https://www.researchgate.net/publication/343539830

10. Pakhale, G., Khosa, R., & Gosain, A. K. (2023). Are flood events really increasing? A case study of Krishna River Basin, India. Natural Hazards Research, 3(3), 374–384. https://doi.org/10.1016/j.nhres.2023.06.007
11. Qiu, J., Cao, B., Park, E., Yang, X., Zhang, W., & Tarolli, P. (2021). Flood monitoring in rural areas of the pearl river basin (China) using sentinel-1 SAR. Remote Sensing, 13(7). https://doi.org/10.3390/rs13071384
12. Rahman, M. R., & Thakur, P. K. (2018). Detecting, mapping and analysing of flood water propagation using synthetic aperture radar (SAR) satellite data and GIS: A case study from the Kendrapara District of Orissa State of India. Egyptian Journal of Remote Sensing and Space Science, 21, S37–S41. https://doi.org/10.1016/j.ejrs.2017.10.002
13. Sarkar, S. (2022). Drought and flood dynamics of Godavari basin, India: A geospatial perspective. Arabian Journal of Geosciences, 15(8). https://doi.org/10.1007/s12517-022-10041-5
14. Tazmul Islam, M., & Meng, Q. (2022). An exploratory study of Sentinel-1 SAR for rapid urban flood mapping on Google Earth Engine. International Journal of Applied Earth Observation and Geoinformation, 113. https://doi.org/10.1016/j.jag.2022.103002
15. Uddin, K., Matin, M. A., & Meyer, F. J. (2019). Operational flood mapping using multi-temporal Sentinel-1 SAR images: A case study from Bangladesh. Remote Sensing, 11(13). https://doi.org/10.3390/rs11131581
16. Vekaria, D., Chander, S., Singh, R. P., & Dixit, S. (2023). A change detection approach to flood inundation mapping using multi-temporal Sentinel-1 SAR images, the Brahmaputra River, Assam (India): 2015–2020. Journal of Earth System Science, 132(1). https://doi.org/10.1007/s12040-022-02020-x
17. Wang, Z., Zhang, C., & Atkinson, P. M. (2022). Combining SAR images with land cover products for rapid urban flood mapping. Frontiers in Environmental Science, 10. https://doi.org/10.3389/fenvs.2022.973192
18. Wu, X., Zhang, Z., Xiong, S., Zhang, W., Tang, J., Li, Z., An, B., & Li, R. (2023). A Near-Real-Time Flood Detection Method Based on Deep Learning and SAR Images. Remote Sensing, 15(8). https://doi.org/10.3390/rs15082046
19. Zhang, H., Qi, Z., Li, X., Chen, Y., Wang, X., & He, Y. (2021). An urban flooding index for unsupervised inundated urban area detection using sentinel-1 polarimetric SAR images. Remote Sensing, 13(22). https://doi.org/10.3390/rs13224511
20. Zhang, L., & Xia, J. (2022). Flood detection using multiple Chinese satellite datasets during 2020 China summer floods. Remote Sensing, 14(1). https://doi.org/10.3390/rs14010051